# Applying the skew-normal distribution to model coherent MPI and to evaluate its impact on PAM signals

Luís G. C. Cancela[a,c], João J. O. Pires[b,c]

[a]*Dep. Information Science and Technology, ISCTE - Instituto Universitário de Lisboa (ISCTE-IUL), Lisbon, 1649-026 Lisboa, Portugal*
[b]*Dep. Electrical and Computer Engineering, Instituto Superior Técnico, Lisbon, 1049-001 Lisboa, Portugal*
[c] *Instituto de Telecomunicações, Lisbon, Portugal*

## Highlights

- Extended skew-normal distribution is used to model the statistics of coherent MPI
- Good agreement between coherent MPI histograms and the ESN statistics is obtained
- The impact of coherent MPI on the performance of PAM signals is studied
- An MPI level of -24 dB is estimated for achieving a 1-dB *Q*-penalty in PAM-4 systems

## Abstract

*We statistically model the coherent multipath interference (MPI) using an extended skew-normal distribution, with the results showing a good agreement with published experimental data. This distribution is very flexible and permits to model data with large skewness values, which is a typical feature in coherent MPI histograms. Furthermore, the developed model was applied to estimate the impact of coherent MPI on PAM-4 systems, with the results showing a 1-dB Q-penalty for an MPI level of -24 dB and a bit error ratio of $10^{-3}$.*

## Keywords

*coherent multipath interference; extended skew-normal distribution; PAM systems; optical communications; Q-penalty; skewness.*

*Email addresses:* luis.cancela@iscte-iul.pt (Luís G. C. Cancela), jpires@lx.it.pt (João J. O.Pires)

*January 29, 2019*

## 1. Introduction

Multipath interference (MPI) is present in a great variety of situations encountered in optical networks and is originated whenever multiple attenuated replicas of a transmitted optical signal propagate over different optical paths and reach the receiver with different delays [1]. The MPI is said to be coherent if the differential delay, *i.e.* the difference in propagation time between the signal and its replicas, is much smaller than the laser source coherence time; otherwise it is considered to be incoherent [2].

In the coherent regime the optical fields propagating over the different paths are correlated, and the amplitude of the received optical power in the presence of coherent MPI has random fluctuations with time scales that typically are much longer than the symbol period. This phenomenon is quite similar to the multipath fading present in wireless communications [1] and, in the same way, it can be a source of burst errors. On the other hand, the time scales of the power fluctuations due to incoherent interference are much shorter than the symbol period and, as a consequence, this impairment is inherently a source of random errors.

The sources of coherent MPI are diverse, ranging from light leakages in WDM optical network nodes [3], to mode coupling in both bend insensitive fibers [4] and few mode fibers [5]. This impairment is particular relevant when the last type of fibers are used in quasi-single-mode operation to explore the large effective area provided by them [5].

A fundamental question, in order to model and evaluate the impact of this impairment, is how to statistically model those slow fluctuations relatively to the symbol period. Contrary to wireless communications, where a large number of statistical models is available to deal with fading [6], in optical communications the research in this subject is incipient and only the Rice and Beta distributions have been proposed in the literature [4, 7]. However, it can be shown that the Rice distribution fails to accurately model the experimental data previously published [3, 4], while the Beta density, although providing a very good fit for the sample data collected from MPI measurement in the context of bend insensitive fibers [4], leads to very poor estimates for the results related to the WDM nodes [8]. These last results were obtained considering a coherent MPI emulator with eight crosstalk paths, all of them with equivalent lengths shorter than the coherence length of the laser source, and the results show a strong asymmetric histogram with heavy left tails. In this work, we explore the use of the skew-normal (SN) distribution [9] to statistically model these results and apply a moment matching method [10] to accurately estimate the distribution parameters from the experimental published data [3]. This distribution, in particular the extended skew-normal (ESN) distribution, is more suitable than both the Rice and Beta distributions, to model data with large skewness values.

Furthermore, we apply the ESN statistics to evaluate the bit-error ratio (BER) of a four level pulse amplitude modulation (PAM-4) system in the presence of coherent MPI. PAM systems are having a renewed interest from the scientific and industrial communities both in datacenter [11-13] and optical access [14] applications. In the first type of application, this modulation scheme can be used for intra-data center interconnections [12], where the short distances involved make the direct detection systems based on PAM signals more attractive than the ones based on coherent detection, as well as for optical

datacenter multicasting [13]. In datacenter interconnection applications MPI is originated from multiple reflections due to poor connectors. This interference is inherently incoherent and its impact on PAM signals has already been analyzed in the literature [15]. However, to the best of our knowledge, no similar studies have been published for coherent MPI, and in this way, this work intends to fill this gap. We note that coherent MPI can be originated, for example, inside of the optical switches used in optical multicasting or in bending-insensitive fibers used in optical access networks.

In this paper, in Section 2, we present the coherent MPI model and in Section 3 we use the ESN distribution, in our model, to statistically characterize the MPI. We then compare our analytical results with the experimental data reported in [3]. In Section 4, we apply the referred ESN distribution to model the coherent MPI in a PAM system and assess the impact of this impairment in a PAM-4 system by computing the BER and the $Q$-penalty for various values of the MPI. Finally, in Section 5, some concluding remarks are drawn.

## 2. Coherent MPI modeling

Consider an optical received signal which is impaired by coherent MPI due to the presence of $N$ multiple propagation paths, and assume that associated with the $i$-th path there is the attenuation factor ${\varepsilon_i}^{1/2}$ and the differential propagation delay $\tau_i$ measured relatively to the signal, in such a way that the MPI level is defined as $\text{MPI} = (\sum_{i=1}^{N} {\varepsilon_i}^{1/2})^2$.

In this scenario and considering that the signal has an arbitrary modulation format, the complex electrical field of the received signal during the symbol interval $[0, T]$ can be represented as

$$E_s(t) = \sqrt{P_o}\, a_s(t)\exp\left[j\left(2\pi\nu_s t + \theta_s(t) + \phi_s(t)\right)\right] + \sum_{i=1}^{N}\sqrt{\varepsilon_i P_o}\, a_s(t-\tau_i)\exp\left[j\left(2\pi\nu_s(t-\tau_i) + \theta_s(t-\tau_i) + \phi_s(t-\tau_i)\right)\right] \quad (1)$$

where $P_o$ denotes the average received optical power in the absence of MPI, $\nu_s$ the signal frequency, $\phi_s(t)$ the laser phase noise, $a_s(t)$ the signal amplitude restricted to the interval $[0, T]$ (zero elsewhere) and $\theta_s(t)$ the signal phase. The first term of the right hand part of Eq. (1) is the field corresponding to the main signal, while the second term is due to the MPI contributions. The behavior and properties of these contributions depend on the laser source coherence time, $\tau_{coh}$.

The MPI is called coherent when the differential propagation delay is smaller than the laser source coherence time, *i.e.* $\tau_i < \tau_{coh}$, and $\tau_i$ is much less than the symbol period, *i.e.* $\tau_i \ll T$, [7]. The first condition implies that $\phi_s(t)$ is correlated with $\phi_s(t-\tau_i)$ and, so, it is reasonable to assume that $\phi_s(t-\tau_i) \approx \phi_s(t)$. Furthermore, the second condition, $\tau_i \ll T$, permits to approximate $\theta_s(t-\tau_i)$ by $\theta_s(t)$ and $a_s(t-\tau_i)$ by $a_s(t)$. It is also assumed that the signal and its replicas are co-polarized. Therefore Eq. (1) can be rewritten as [7],

$$E_s(t) = \sqrt{P}\, a_s(t)\exp\left[j\left(2\pi\nu_s t + \theta_s(t) + \phi_s(t)\right)\right] \quad (2)$$

with

$$P \approx P_o|1 + \sum_{i=1}^{N} \sqrt{\varepsilon_i} \exp(-j\varphi_i)|^2 \quad (3)$$

where $\varphi_i = 2\pi\nu_s\tau_i$ is the phase offset of the $i$-th interfering field due to multipath propagation relative to the signal. The phase offset varies in a random manner, as a consequence of a number of uncontrollable disturbances, like drifts in the source central frequency, variations in the differential delay coming from mechanical and thermal fluctuations, as well as from variations in the refractive index, when the MPI is originated from mode coupling. In this case, $P$ is no longer constant and it is subject to slow fluctuations of random nature. Owing to the correlation between the optical fields, the random variables $\varphi_i$ are not independent, as it is the case of incoherent crosstalk [7]. In this last case, the summation in Eq. (3) corresponds to the sum of $N$ independent and identically distributed (i.i.d.) random variables, and assuming the same attenuation factor for all the interferers it can be rewritten as

$$P \approx P_o + 2P_o\sqrt{MPI}X \quad (4)$$

where $X$ is a random variable given by

$$X = \frac{1}{N}\sum_{i=1}^{N} cos\ \varphi_i \quad (5)$$

where $\varphi_i$ is a uniformly distributed random variable over the interval $[0, \pi]$ and $X$ tends to a Gaussian distributed random variable with zero mean as the number of interferers increase. In the presence of correlation, the i.i.d. assumption no longer holds and as a consequence the statistics of $X$, as well as the statistics of the power fluctuations are difficult to predict and so the problem of finding an adequate probability density function (PDF) to describe these random fluctuations is not tractable in an easy way. Our approach to face this problem is to estimate the PDF of the MPI from the experimental data given in [3]. For that purpose, we choose a sufficiently flexible distribution, like the extended skew-normal (ESN) [9] to model that data, and a moment matching method to estimate the distribution parameters [10]. Before proceeding with the statistical characterization of the instantaneous received optical power $P$ we rewrite Eq. (4), in a more general form [5], as

$$P = P_0 + \Delta P(X - \eta_X)\ , \quad (6)$$

where $X$ is a continuous random variable to be characterized in the next section, $\eta_x$ is the mean of $X$ and $\Delta P = bP_o\sqrt{\mathrm{MPI}}$, with $b$ being a constant to be estimated in the next section, which accounts for the fact of the random variables in Eq. (3) not being anymore i.i.d.

It is worth to note that the condition $\tau_i \ll T$ can impose a limit on the maximum transmission rate for which this model can be applied. As a consequence, the differential delays between the signal and its replicas must be very small in the sense that can only be observed when using integrated OXCs (optical cross-connects) [16]. As an example, for a baud rate of 25 Gbaud ($T$=0.04 ns) the differential lengths between the signal and its replicas must be much smaller than 8 mm.

## 3. Statistical distribution used for MPI characterization

The SN distribution is a generalization of the normal distribution to which a shape parameter ($\alpha$) has been added to regulate the skewness of the distribution. On the other hand, the ESN distribution is obtained from the SN distribution by introducing a new parameter $\tau$, called truncation parameter [17], and has the advantage of permitting to model data with larger values of skewness than the SN distribution [9]. The effect of the $\tau$ is not independent of the one of $\alpha$, and both the parameters influence the skewness as well as the kurtosis of the distribution. In order to get some insight into the problem let's consider a continuous random variable $X$ having the following PDF [9]:

$$f_X(x\,;\alpha\,;\tau) = \varphi(x)\frac{\Phi(\tau\sqrt{1+\alpha^2}+\alpha x)}{\Phi(\tau)}\,, \tag{7}$$

where $\varphi(x)$ is the standard normal density function, and $\Phi(\alpha x)$ is the cumulative distribution function of $\varphi(x)$ evaluated at $\alpha x$. Therefore, the random variable $Y = \xi + \omega X$, with location parameter $\xi$, the scale parameter $\omega$, has an ESN distribution with the parameters ($\xi$, $\omega$, $\alpha$, $\tau$), which can be described as $Y \sim \mathrm{ESN}(\xi, \omega^2, \alpha, \tau)$. The first four moments of the random variable $Y$, the mean, variance, skewness and excess kurtosis (*i.e.* the distribution kurtosis minus 3, which is the kurtosis value from the Gaussian distribution) can then be found, respectively, as follows [9, page 39],

$$\eta_Y = \xi + \zeta_1(\tau)\omega\delta\,, \tag{8a}$$

$$\sigma_Y^2 = \omega^2\{1 + \zeta_2(\tau)\delta^2\}\,, \tag{8b}$$

$$\gamma_{1Y} = \frac{\zeta_3(\tau)\delta^3}{\{1+\zeta_2(\tau)\delta^2\}^{3/2}}\,, \tag{8c}$$

$$\gamma_{2Y} = \frac{\zeta_4(\tau)\delta^4}{\{1+\zeta_2(\tau)\delta^2\}^{2}}\,, \tag{8d}$$

with $\delta = \alpha/\sqrt{1+\alpha^2}$ and the functions $\zeta_i(\tau)$ with $i = 1,\ldots,4$ defined in [9, page 30].

Assuming, now, that $P$, given by Eq. (6), is described by an ESN statistic, then its PDF can be written as

$$f_P(p\,;\alpha\,,\tau) = \frac{1}{bP_0\sqrt{\mathrm{MPI}}} f_X\left(\frac{\frac{p}{P_0}-1+b\eta_X\sqrt{\mathrm{MPI}}}{b\sqrt{\mathrm{MPI}}}\,;\alpha\,,\tau\right), \tag{9}$$

where $f_X(x\,;\alpha\,,\tau)$ is the PDF of $X$ given by Eq. (7). The PDF of $P$ can also be written in terms of the $Q$ parameter, knowing that $Q = P/2\sigma$, where $\sigma^2$ is the variance of the receiver noise,

$$f_Q(Q;\alpha,\tau) = \frac{1}{b\bar{Q}\sqrt{\mathrm{MPI}}} f_X\left(\frac{Q/\bar{Q}-1+b\eta_X\sqrt{\mathrm{MPI}}}{b\sqrt{\mathrm{MPI}}}\,;\alpha,\tau\right), \tag{10}$$

with $\bar{Q} = P_0/2\sigma$, being the $Q$ parameter without MPI. Therefore, we can write that $Q \sim \text{ESN}(\xi, \omega^2, \alpha, \tau)$, where $\omega = b\bar{Q}\sqrt{\text{MPI}}$ and $\xi = \bar{Q}(1 - b\sqrt{\text{MPI}}\eta_X)$.

Using the formulas given in Eq. (8a) through Eq. (8d) it is also possible to obtain the four theoretical moments of $Q$: the mean $\eta_Q$, the variance $\sigma_Q^2$, the skewness $\gamma_{1Q}$, and the excess kurtosis $\gamma_{2Q}$ as a function of the parameters $b$, $\eta_X$, $\alpha$ and $\tau$ that appear in Eq. (10). The parameter $b$ can then be found by knowing that $\sigma_Q^2 = \omega^2\{1 + \zeta_2(\tau)\delta^2\}$, so

$$b = \frac{\omega}{\bar{Q}\sqrt{\text{MPI}}} = \frac{\sqrt{\frac{\sigma_Q^2}{1+\zeta_2(\tau)\delta^2}}}{\bar{Q}\sqrt{\text{MPI}}}. \tag{11}$$

Likewise, the parameter $\eta_X$ can be found by knowing that $\eta_Q = \xi + \zeta_1(\tau)\omega\delta$, so

$$\eta_X = -\frac{\eta_Q - \zeta_1(\tau)\omega\delta - \bar{Q}}{b\bar{Q}\sqrt{\text{MPI}}}. \tag{12}$$

Furthermore, it is also possible to find a pair of parameters $(\alpha, \tau)$ by knowing the skewness $(\gamma_{1Q})$ and excess kurtosis $(\gamma_{2Q})$ of the $Q$ parameter.

We are now in conditions to verify the appropriateness of the distribution of $Q$ given by Eq. (10) to model the experimental data given in [3]. We use a moment matching method to estimate the parameters $\alpha$, $\tau$, $\eta_X$ and $b$ present in Eq. (10) [10]. According to this method the mean $\bar{x}$, the variance $s^2$, the skewness $\gamma_1$, the excess kurtosis $\gamma_2$ of the samples, computed from the set of experimental data samples $\{x_i\}_{i=1}^n$ (we used $n = 100$ samples), are equated to the correspondent theoretical parameters of the distribution of $Q$, *i.e.* $\eta_Q = \bar{x}$, $\sigma_Q^2 = s^2$, $\gamma_{1Q} = \gamma_1$, and $\gamma_{2Q} = \gamma_2$. Using the data from [3], that has been obtained for $\bar{Q} = 6$ (which was determined from a receiver sensitivity of -34 dBm at a BER=$10^{-9}$, considering the transmission of 2.5 Gb/s non-return-to-zero signals (NRZ) [3]) and $MPI = -30$ dB, we get $\bar{x} = 5.516$, $s = 0.312$, $\gamma_1 = -1.431$, and $\gamma_2 = 2.73$. As seen, the sample data exhibits an excess kurtosis of 2.73 which indicates that the PDF tails asymptotically approach zero more slowly than a Gaussian distribution characterized by a zero excess kurtosis, and a quite large skewness absolute value (1.431), which is an indication of a highly asymmetric distribution. This behavior is a clearly indication that distributions like the Beta and SN, although being appropriate to describe negative tails, cannot be used in this case because they are not able to model skewness absolute values larger than 1, as shown in [8] for the Beta distribution scenario.

The next, and final, step in order to find the suitable ESN distribution to model the data from [3] is just to compute an estimate of the parameters $b$ and $\eta_X$ that appear in Eq. (10), by using Eq. (11) and Eq. (12), respectively. We have obtained $b = 4.83$ and $\eta_X = 1.82$. Furthermore, it is also possible to find, by a trial and error method, a pair of estimates parameters $(\alpha, \tau)$ that guarantee $\gamma_{1Q} = \gamma_1$ and $\gamma_{2Q} = \gamma_2$. For example, the pair $(-13.51, -1.985)$ leads to the $\gamma_{1Q} = -1.431$ and $\gamma_{2Q} = 2.73$, which were referred before, in the previous paragraph.

In Fig. 1, it is plotted the experimental histogram given in [3], with the data represented by the red crosses, as a function of the $Q$ parameter, as well as the PDF

$f_Q(Q\,;\alpha\,,\tau)$, given by Eq. (10), for different values of $\tau$, $\alpha = -13.51$ and $MPI = -30$ dB. These PDFs, as described in the previous paragraphs, are computed from the first four sample moments (mean, variance, skewness and excess kurtosis) with an estimate of the parameters $b$ and $\eta_X$ obtained from Eq. (11) and Eq. (12), respectively, and an estimate of the parameters pair $(\alpha, \tau)$ that guarantee $\gamma_{1Q} = \gamma_1$ and $\gamma_{2Q} = \gamma_2$. As can be seen, the quality of the fitting is quite good for $\tau = -1.985$, which is expected since this PDF is computed from the sample moments of the experimental histogram. On the other hand, the PDF for $\tau = 0$, with the same estimates for $b$, $\eta_X$ and $\alpha$ used in the previous scenario, which corresponds to the SN case, leads to the worst fit, especially in the falling edge and in the peak of the curves.

In Fig. 2 the PDF $f_Q(Q\,;\alpha\,,\tau)$ is plotted again as a function of the $Q$ parameter, but for different values of $\alpha$ using $\tau = -1.985$ and the other estimated parameters, $b$ and $\eta_X$. As in Fig.1 the best fitting occurs for the parameters estimated from the sample moments of the experimental histogram, *i.e.* $\alpha = -13.51$ and $\tau = -1.985$. It can, also, be observed that when the absolute value of $\alpha$ increases the PDF becomes more peaked. On the other hand, when this value decreases the PDF right tail widens.

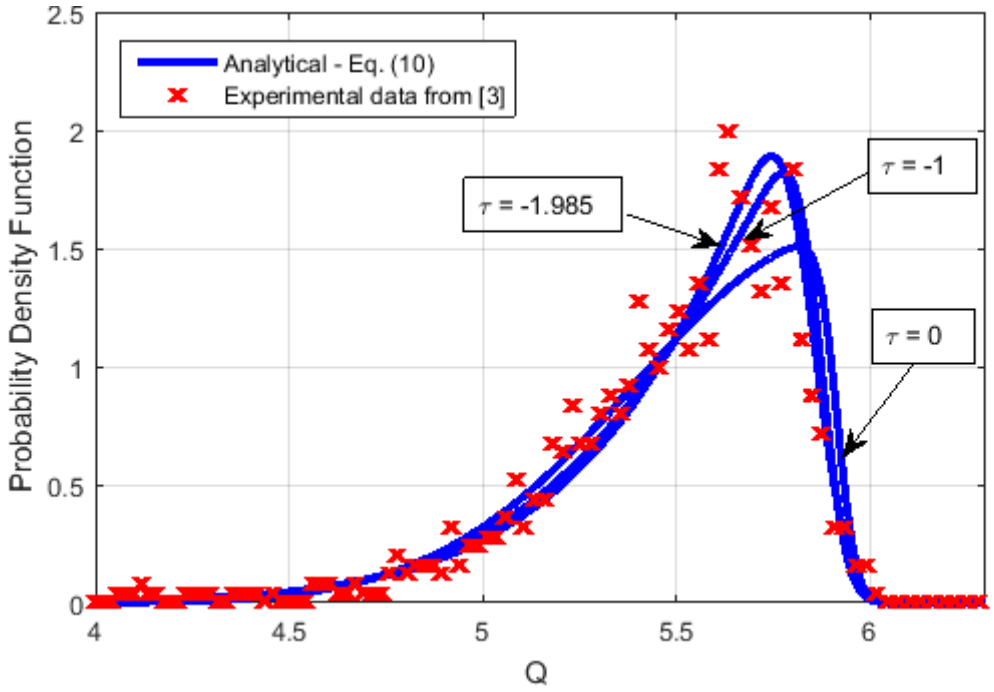


**Fig. 1:** PDF of the $Q$ parameter for different values of the parameter $\tau$ with MPI=-30 dB and $\alpha = -13.51$. The experimental data obtained from [3] is also represented.

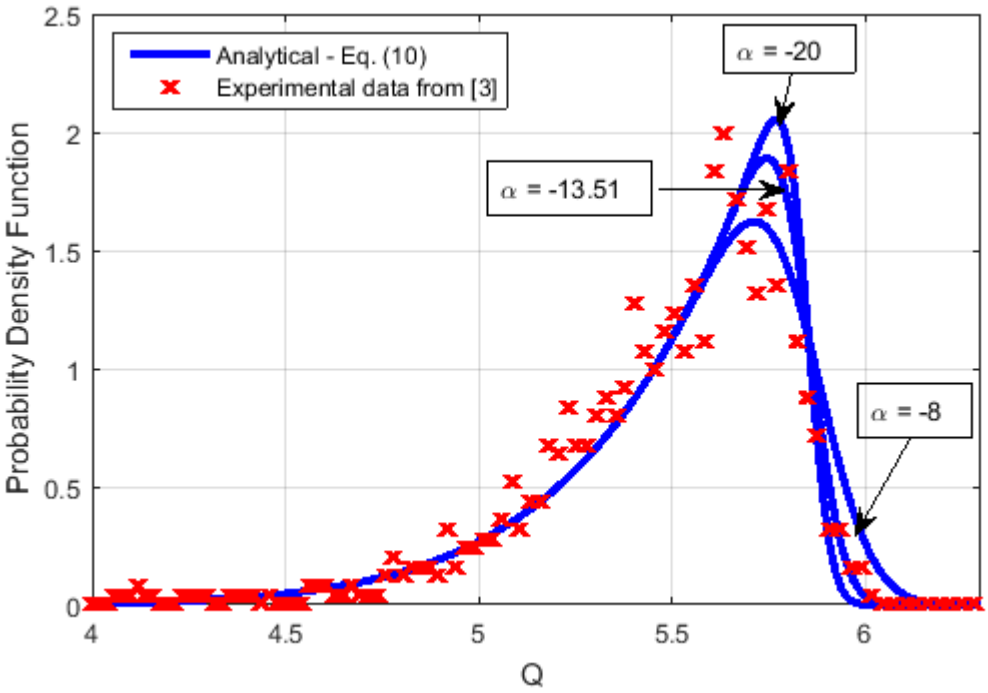


**Fig. 2:** PDF of the $Q$ parameter for different values of the parameter $\alpha$ with MPI=-30 dB and $\tau = -1.985$. The experimental data obtained from [3] is also represented.

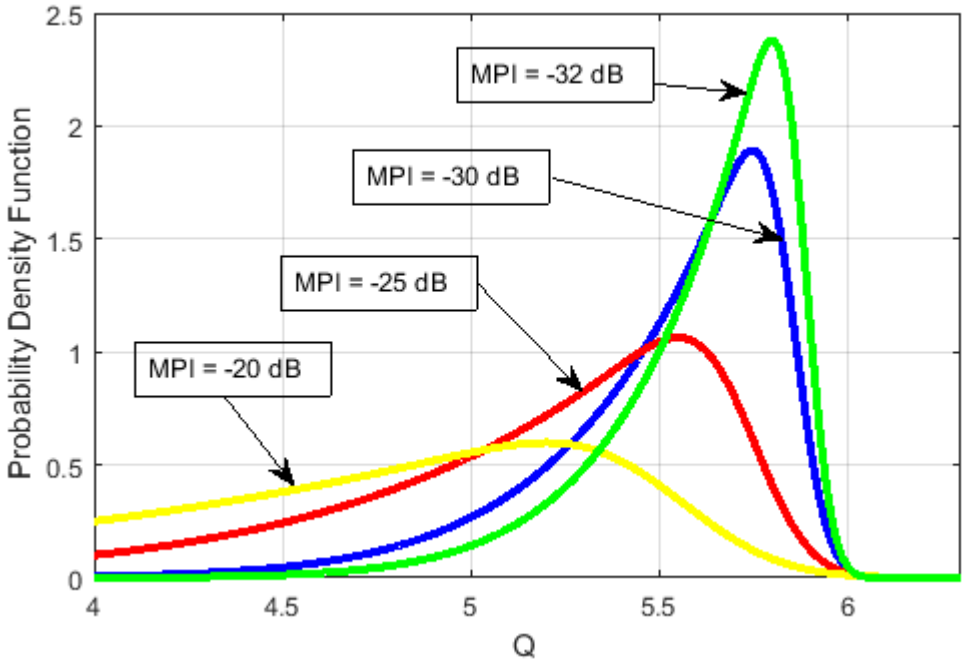


**Fig. 3:** PDF of the $Q$ parameter for different values of MPI, with $\alpha$ = -13.51, and $\tau$ = -1.985.

Using the previously obtained parameters that characterize the distribution of $Q$ it is now possible to understand how the MPI values affect the PDF shape. Fig. 3 shows the PDF of the $Q$ parameter for different values of MPI (-20, -25, -30 and -32 dB) considering

$\alpha = -13.51$, and $\tau = -1.985$, which are the values obtained from the sample moments of the experimental histogram. It can be observed from Fig. 3 that the MPI variation deeply impacts the shape of the PDF curves. These curves become less peaked and broader for increasing values of MPI, what potentially contributes to degrade the system performance, as we will analyze in the next section. On the opposite way, for decreasing values of MPI, the PDF shape become more peaked and narrower, and in the limit when there is no MPI impact the value of the $Q$ parameter tends to 6, in accordance with the data from [3].

In order to compare the fitness of different statistical distributions to model the type of MPI under study, it is plotted in Fig. 4 the PDF of the ESN distribution, as well as the Beta and Rician distributions for a $MPI = -30$ dB. The experimental data obtained from [3] is also represented. The ESN distribution uses the parameters $\tau = -1.985$ and $\alpha = -13.51$, that better approximate the experimental histogram, as discussed previously. Likewise, the Beta and Rician distributions parameters are chosen to mimic the histogram. The PDF of the $Q$ parameter when the Beta distribution is used to model the coherent MPI is obtained from [8], with the parameters $\alpha = 2.24$, and $\beta = 1.41$. In the same way, the PDF of the $Q$ parameter when the Rician distribution is used to model the coherent MPI is obtained from [7]. From Fig. 4 we can observe that the Rician distribution is clearly not appropriate to describe neither the left nor the right tail of the histogram. In what concerns the Beta distribution, although describing better the histogram right tail, it also clearly fails to describe the left tail of the histogram.

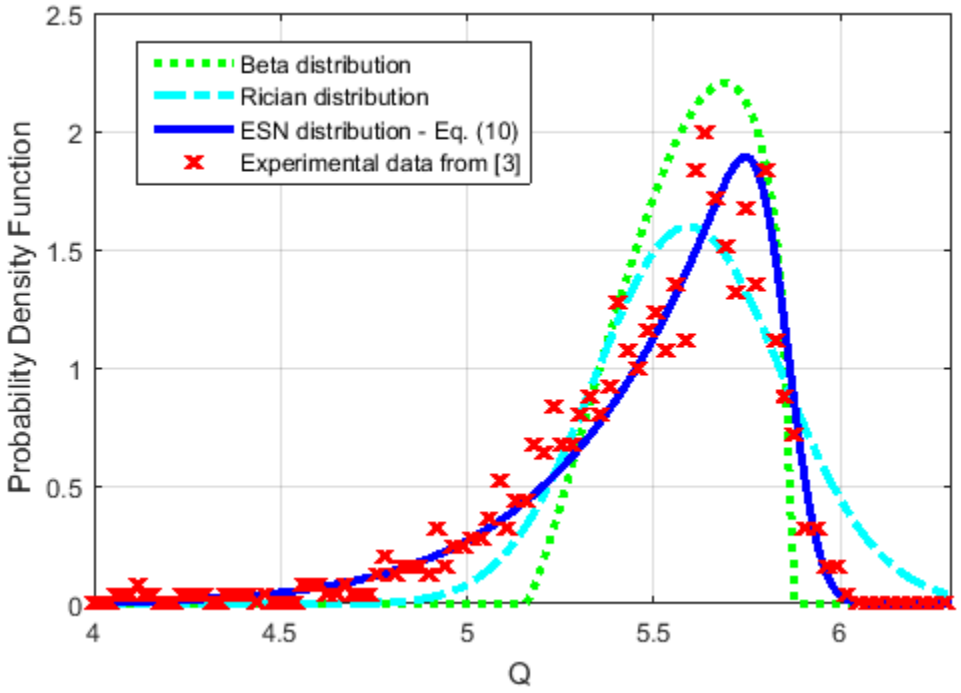


**Fig. 4**: PDF of the $Q$ parameter obtained with ESN, Beta and Rician statistics for $MPI = -30$ dB. The experimental data obtained from [3] is also represented. The ESN distribution uses $\tau = -1.985$ and $\alpha = -13.51$, and the Beta distribution uses $\alpha = 2.24$, and $\beta = 1.41$ [8].

## 4. Impact of coherent MPI on the performance of a PAM system

In this section we illustrate how the MPI modelled by the ESN distribution, described in the previous section, impacts the system performance in a PAM system. We start the analysis with the well-known formula for the BER for a PAM-M system without MPI, which is given by [18],

$$BER_{without\ \mathrm{MPI}} = \frac{M-1}{M}\frac{1}{log_2 M}\,\mathrm{erfc}\left(\sqrt{\frac{3log_2 M}{(M^2-1)}Q}\right), \tag{13}$$

where $M$ is the number of symbols, erfc(.) is the complementary error function, and $Q$ is the $Q$ parameter.

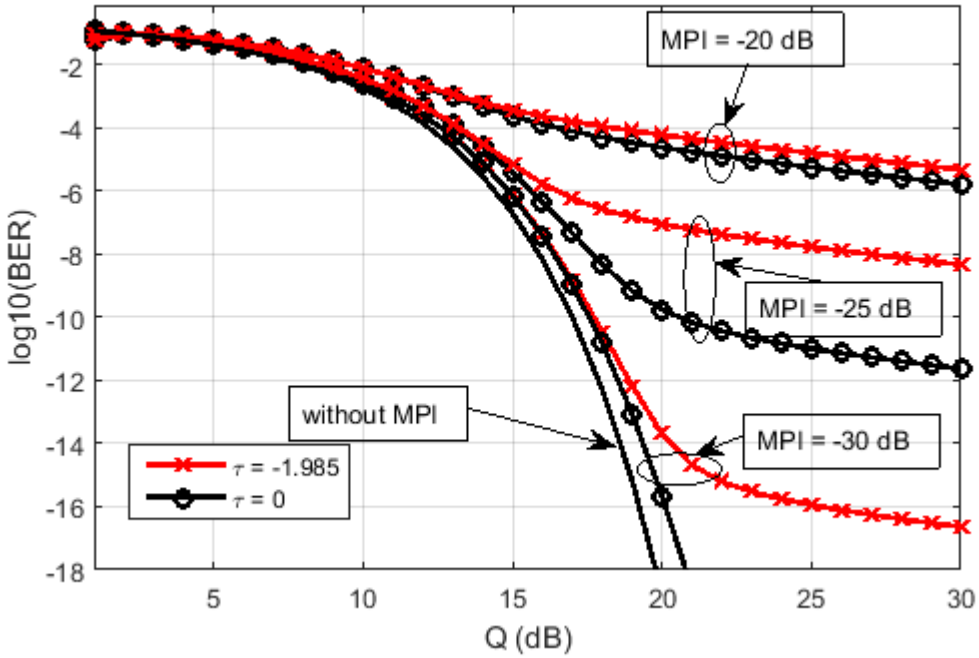


**Fig. 5:** BER of a PAM-4 system as a function of the $Q$ parameter for SN (τ = 0) and ESN (τ = -1.985) distributions with $\alpha$ = -13.51, considering 4 values of the MPI level, without MPI, -30 dB, -25 dB and -20 dB.

In the presence of MPI Eq. (13) must be modified leading to

$$BER = \frac{M-1}{M}\frac{1}{log_2 M}\int_0^{\infty}\mathrm{erfc}\left(\sqrt{\frac{3log_2 M}{(M^2-1)}Q}\right) f_Q(Q;\alpha,\tau)dQ\,, \tag{14}$$

where $f_Q(Q;\alpha,\tau)$ is the PDF of the MPI given by Eq. (10). Note that a similar analytical formalism was also used in [19], but for assessing the impact of the atmospheric turbulence in PAM systems.

In order to quantify the effect of the MPI in a PAM system we focus our analysis on a PAM-4 system, which is commonly used in datacenter and optical access applications [11-

15]. Using Eq. (14), in combination with the estimated parameters explained in Section 3, one can obtain the results depicted in Fig. 5 for four values of the MPI level (without MPI, -20, -25 and -30 dB). Note that, despite the parameters used in Eq. (14) are obtained considering NRZ signals, we have assumed here that the statistic of the coherent MPI for the PAM-4 formats is the same, since for a given differential delay $\tau_i$ and the same bit rate, the condition $\tau_i \ll T$ is easily verified in PAM systems due to larger symbol periods. The results from Fig. 5 confirm the previous predictions, *i.e.* the BER degrades significantly when the MPI increases, resulting even in the appearance of error floors in the curves. Another relevant conclusion, we can get from this figure, is that the SN model (*i.e.* $\tau = 0$) significantly underestimate the MPI impact on the BER performance, especially in the error floor region. Note that the curve without MPI can also be obtained with Eq. (13) and is a well-known curve that states that for a BER= $10^{-3}$ the *Q* parameter must be 11.2 dB [18].

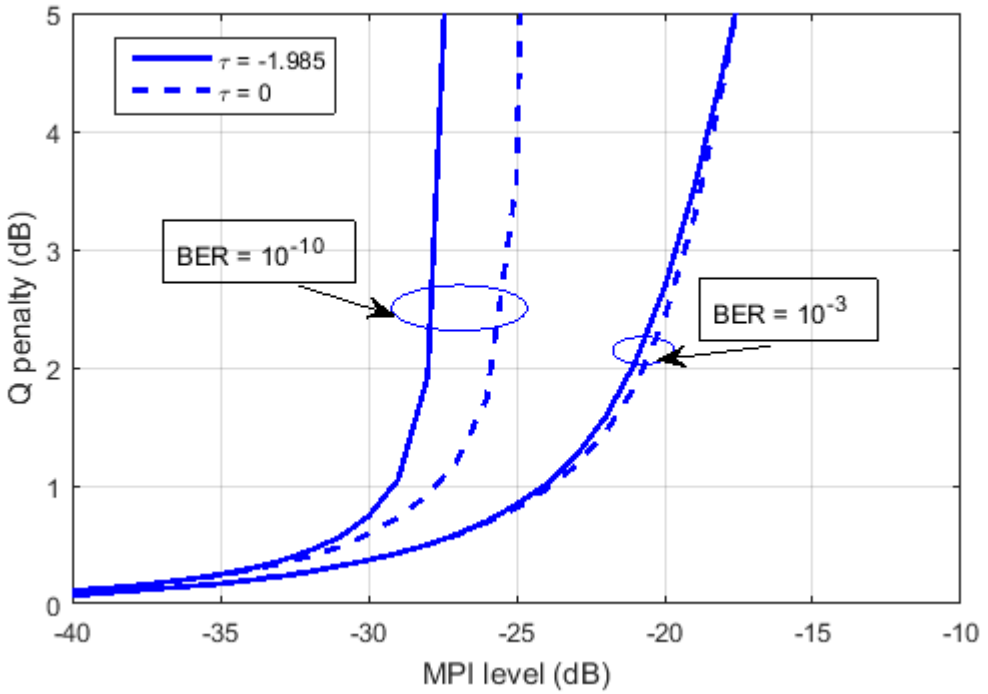


**Fig. 6:** *Q*-penalty (@ BER= $10^{-3}$ and BER= $10^{-10}$) as a function of the MPI level for PAM-4 systems considering the ESN and SN distributions.

In Fig. 6 the *Q*-penalty (@ BER= $10^{-3}$ and BER= $10^{-10}$) is plotted as a function of the MPI level for a PAM-4 system, considering the SN and ESN models. For a BER=$10^{-3}$ the discrepancy between the results of the SN and ESN models is almost negligible, but for BER=$10^{-10}$, which corresponds to the floor region in Fig. 5, the first model predicts an MPI value about 1.5 dB higher than the second one for a 1-dB penalty, which means that the SN model is more tolerant to MPI. We also observe that for a BER=$10^{-3}$ an MPI level of -24 dB provides a penalty of 1 dB and this penalty doubles for an MPI level 3 dB higher (*i.e.* -21 dB). On the other hand, for a BER=$10^{-10}$, an MPI level of -29 dB is needed for a 1dB *Q*-penalty for the ESN model, whereas for an MPI of -28 dB this penalty is already 2 dB. As a final remark, we note that the impact of coherent MPI in a PAM-4 system is less harmful than the one imposed by incoherent MPI, which was analyzed in [15]. In the referred study the authors concluded that for a 1 dB penalty the incoherent MPI should be

-30 dB (@BER=$10^{-3}$), so there is a 6 dB penalty difference between these two impairments.

## 5. Conclusions

In this work we have investigated the problem of statistically modelling the optical power fluctuations due to coherent MPI in optical communications systems. We have used the ESN distribution to perform this task because it provides very good estimates for experimental data with highly asymmetric behavior and consequently with large skewness values, which are typical in a WDM optical network node scenario [3]. Other distributions, like the Rice and Beta distributions, have been tested in prior works to model the coherent MPI, but none of them have the flexibility in terms of the capacity to describe asymmetric behaviors like the ESN described in this paper.

The developed model, based on the ESN statistics, has been used to assess the impact of coherent MPI on the performance of PAM signals, by being able to predict the BER and the *Q*-penalty due to this impairment. The results obtained revealed that the BER degrades significantly when the coherent MPI increases, and the appearance of error floors in the BER curves is noticed. We have also found that for a *Q*-penalty of 1 dB (@BER= $10^{-3}$) the MPI level should be at most -24 dB for a PAM-4 system.

**Funding:** This work is funded by FCT/MCTES through national funds and when applicable co-funded EU funds under the project UIDB/EEA/50008/2020.

## References

[1] S. Ramachandran, J. Nicholson, S. Ghalmi, and M. Yan, Measurement of multipath interference in the coherent crosstalk regime, IEEE Photon. Technol. Lett. 15 (8) (2003) 1171-1173.
[2] A. Arie, M. Tur, and E. Goldstein, Probability-density function of noise at the output of a two-beam interferometer, J. Opt. Soc. Am. A, 8 (12) (1991) 1936-1942.
[3] C. Yu, System degradation due to multipath coherent crosstalk in WDM network nodes, J. Lightw. Technol. 16 (8) (1998) 1380-1386.
[4] M. Travagnin, BER penalty induced by coherent MPI noise in FTTH optical links, J. Lightw. Technol. 31 (18) (2013) 3021-3031.
[5] J. Downie, Quasi-Single-Mode Fiber transmission for optical communications, J. Sel. Top. Quantum Electron 23 (3) (2017) 4400312.
[6] M. Simon and M. Alouini, Digital communications and fading channels, Wiley Interscience, 2nd ed., 2005.
[7] J. Pires and L. Cancela, Theoretical insights into the impact of coherent and incoherent crosstalk on optical DPSK signals, J. Lightw. Technol. 28 (19) (2010) 2766-2774.
[8] L. Cancela and J. Pires, How to statistically model coherent MPI on optical communications?, in: Proc. OSA Advanced Photonics Congress 2018, Zurich, 2018, Paper SpM3G.3.
[9] A Azzalini, The skew-normal and related families, Cambridge University Press, 2014.
[10] S. AbouRizk, D. Halpin, J. Wilson, Fitting Beta distributions based on sample data, Journal of Construction Engineering and Management, 120 (2) (1994) 288-305.
[11] K. Szczerba, P. Westbergh, J. Karout, J. Gustavsson, A. Haglund, M. Karlsson, P. Andrekson, E. Agrell, and A. Larsson, 4-PAM for high-speed short-range optical communications, J. Opt. Commun. Netw. 4 (11) (2012) 885-894.
[12] X. Zhou, H. Liu, R. Urata, and S. Zebian, Scaling large data center interconnects: challenges and

solutions, Optical Fiber Technology 44 (2018) 61-68.
[13] H. Rastegarfar, L. Yan, K. Szczerba, and E. Agrell, PAM performance analysis in multicast-enabled wavelength-routing data centers, J. Lightw. Technol. 35 (13) (2017) 2569-2579.
[14] S. Barthomeuf, F. Saliou, L. Neto, P. Chanclou and D. Erasme, TDM-PON PAM downstream transmission for 25 Gbit/s and beyond, Photonics, 5 (45) (2018) 1-9.
[15] C. Fludger, M. Mazzini, T. Kupfer, and M. Traverso, Experimental measurements of the impact of multi-path interference on PAM signals, in: Proc. OFC 2014, USA, 2014, Paper W1F.6.
[16] K. Ueda, Y. Mori, H. Hasegawa, K.-I. Sato, and T. Watanabe, Large-scale optical-switch prototype compactly implemented with novel functional configuration, in: Proc. OFC 2015, USA, 2015, Paper W3D.1.
[17] A. Seijas-Macias, A. Oliveira, and T. Oliveira, The presence of distortions in the extended skew-normal distribution, in: Proc. 2nd ISI Regional Statistics Conference 2017, Indonesia, 2017, Paper IPS21.
[18] J. Proakis, Digital communications, McGraw Hill, 3rd ed., 1995.
[19] H. Yao, X. Ni, C. Chen, B. Li, X. Zhang, Y. Liu, S. Tong, Z. Liu, and H. Jiang, Performance of M-PAM FSO communication systems in atmospheric turbulence based on APD detector, Optics Express 26 (18) (2018) 23819-23831.